Proceedings of the Institute of Acoustics

TEMPORAL VARIABILITY OF HIGH FREQUENCY SEAFLOOR ACOUSTIC BACKSCATTER FROM A SANDY SITE IN THE GULF OF MAINE

Kaan Cav	Center for Coastal & Ocean Mapping, University of New Hampshire
Jenna Hare	Center for Coastal & Ocean Mapping, University of New Hampshire
Anthony Lyons	Center for Coastal & Ocean Mapping, University of New Hampshire
John Hughes-Clarke	Center for Coastal & Ocean Mapping, University of New Hampshire

1 INTRODUCTION

Active sonar systems are used for many remote sensing applications such as hydrography, seafloor characterization, and target detection. The effective use of these sonar systems is dependent on a robust understanding of the seafloor acoustic response. Previous work has focused on the dependence of backscattering strength (SS) on sediment type, grazing angle, and frequency, however the temporal variability of SS has not been studied as extensively[6,15]. Two studies that have investigated temporal variability only spanned weeks and did not report SS time series, instead decorrelation methods were used to track temporal variability[10,5]. Another experimental study investigated how biological activity affected SS over a period of 60 days by introducing animals (e.g. tethered crabs, mollusks, fish, cockle) within the acoustic footprint of the transducer[14]. Jumars et al.[11] investigated a silty area off the coast of Northern California and observed a circadian pattern in temporal SS variability over a period of 49 days that was most likely driven by benthic change.

High energy events that occur on various timescales (seconds to years) are known to alter the parameters that affect SS[4,9]. Seafloor roughness is an important driver of temporal SS change[12]. For example, near bed hydrodynamics caused by storms can alter seafloor roughness. Biological activity (bioturbation) can both create and destroy roughness elements (e.g smoothing sharp features, reducing bedform heights, deposit feeding)[3,9]. Seasonal changes occurring on time spans of days to months can be caused by environmental factors such as the presence of sea grass[13].

This work builds upon previous studies conducted by Catoire[4] and Hare et al.[7]. Research presented here focuses on the analysis of temporal variations in SS observed from a stationary tripod located in a shallow water, sandy region at the mouth of the Piscataqua River, New Hampshire, USA. The data spans the winter of 2022-2023, covering temporal variability of SS on timescales of hours to months. Increasing our understanding of the environmental parameters that drive changes in SS can inform future remote sensing applications, improve model implementation, and support the development of new multibeam calibration techniques.

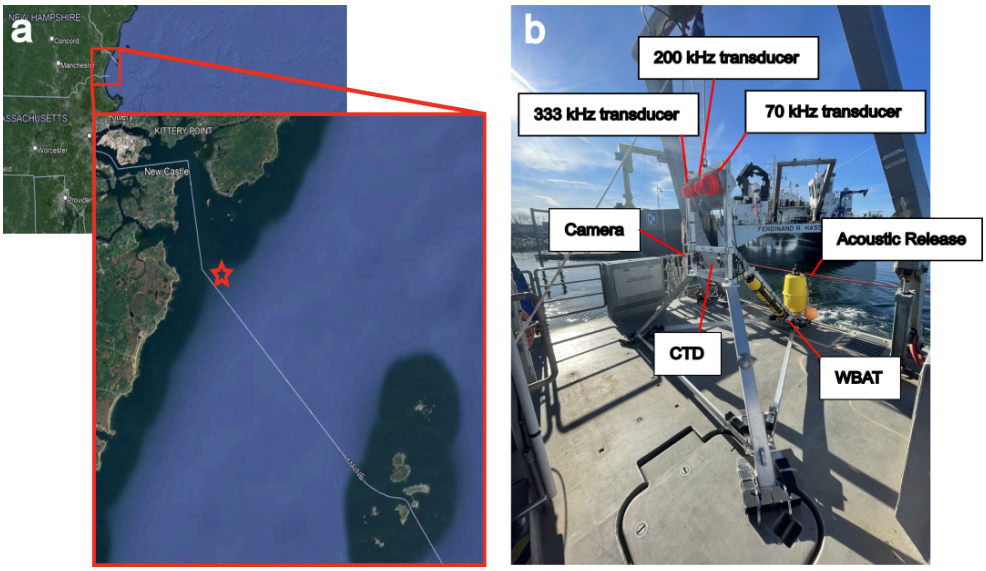

Figure 1: (a) Map showing tripod location (red star) (b) Instruments mounted to custom-made tripod

2 METHODS

2.1 Equipment

Data were collected using a stationary platform on the seafloor in the Gulf of Maine near the mouth of the Piscataqua River (Fig. 1a). The deployment was from December 2022 to May 2023. The average depth of the study site was 16 m. Previous research[15] found the area to be sandy with median grain sizes ranging between 0.088 mm and 0.125 mm. The platform was a custom-built tripod[4] (Fig. 1b), with a height (h) of 2.12 m. The tripod was equipped with three transducers that operated at 70 kHz, 200 kHz, and 333 kHz having beam widths of 18°, 7°, and 7°, respectively. Only the 70 kHz transducer was used as a split beam. The transducers were controlled by a SIMRAD Wide Band Autonomous Transceiver (WBAT). Fifty pings with a pulse length of 256 μs were transmitted on the hour, every hour. The tripod was also equipped with a CTD to collect environmental measurements (e.g. temperature, salinity, significant wave height). An Olympus TG-6 underwater camera provided photographs of the seafloor for the first 30 days of the deployment. The photographs of the seafloor show the presence of shell pieces and small bedforms. The transducers are mounted to the tripod so that the grazing angle of their main beams' with respect to a flat seafloor would be 20°. The geometry of the tripod allowed us to study a patch of the seafloor that spanned 4 m to 11 m in front of the tripod with the 70 kHz transducer and 4.9 m to 7.2 m with the narrower beam width of the 333 kHz transducer.

2.2 Data Processing

The power of the scattered field received by the transducer was internally calculated by the WBAT[2]. Transducer beam widths were accounted for based on values provided by the manufacturer. The sound intensity levels of the 50 pings were averaged. Scattering strength (S_b) was then calculated using the averaged sound intensity level for each hour and applying area corrections (A), beam corrections (BP)

and transmission losses (TL) as seen in Eq. 1.

$$S_b = RL - SL - 2BP + 2TL - 10\log_{10} A \tag{1}$$

Slant range (R) was computed using two way travel time and the measured sound speed. Horizontal range (x) was computed using $x = \sqrt{R^2 - h^2}$.

During stormy periods, the acoustic response of the seafloor was sometimes masked, likely due to bubbles or suspended sediment. The data were assessed for loss of seafloor acoustic response using the measured phases from the split beam transducer. For every ping, the phase differences of the split beam were computed. The standard deviation of the phase differences (σ) among the 50 pings was calculated and from that an average of σ from 4-10 m slant range was taken ($\bar{\sigma}$). Periods of high $\bar{\sigma}$ coincided with storm events. Data above a specified threshold of 0.28 for $\bar{\sigma}$ were rejected. After periods that lacked seafloor acoustic response were removed, 56% of the data remained.

When analyzing the phase data from the split beam, a sudden shift in the physical echo arrival angles was observed likely due to settling of the tripod. The physical echo arrival angles relative to the main beam axis were computed from the phase data[2]. The physical echo arrival angles in the fore/aft direction (θ) were used. A shift in θ coincided with a large storm event on March 14$\hat{\text{t}}$h, 2023. For the period prior to the storm and following the storm, an average of the physical echo arrival angles ($\overline{\theta}$) were taken. Outliers were removed from the phase data where the difference between $\overline{\theta}$ and θ was greater than 2°. The remaining acoustic data was smoothed and then a one day moving average was applied. For every hour, the grazing angle of the transducer's main beam axis with respect to a flat seafloor, $\theta_{MB}(t)$, was computed from a non-linear least squares fit of θ to $sin^{-1}(\frac{h}{R}) - \theta_{MB}$. The best fit yielded values of $\theta_{MB}(t)$ ranging from 19.3° to 20.6° (with R^2 greater than 0.98), comparable to the tripod design value of 20°. The average of the transducers' main beam angle with respect to a flat seafloor ($\overline{\theta_{MB}}$) from before and after the shift was 20.2° and 19.5°, respectively.

SS is defined as an ensemble average of uncorrelated samples[9]. In order to maintain a $\pm$1.25 dB and 85% confidence interval[4], a 25 point averaging window was used[1]. The grazing angle (θ_g) was corrected for the shift using $\overline{\theta_{MB}}$. When defining the window, a θ_g of interest was chosen (e.g. 10°) and a window centered around that θ_g was defined. S_b values at each grazing angle within the window were averaged, yielding SS. This spatial averaging method assumes that SS does not change drastically over the spatial area being averaged. The range of θ_g being averaged to compute $SS(\theta_g)$ was not overlapping.

To determine whether the SS values are being biased by the 25 point spatial averaging process, an analysis was done using the small slope approximation (SSA) roughness scattering model[8]. Using the same grazing angles as the data, SS values were modeled for 70 kHz using the SSA model with the 'medium sand' parameters[8] ($a_p = 1.845, v_p = 1.1782, \delta_p = 0.01624, \gamma_2 = 3.25, w_2 = 1.406e-4, \gamma_3 = 3.0, w_3 = 3.59e-4, v_t = 0.002, \delta_t = 1.0$). Averages over a 25 point sliding window were computed for all grazing angles of interest (8°-22°) (Fig. 2). Results of this analysis showed that a minimal error of 0.05 dB - 0.25 dB would be introduced by this averaging scheme.

3 RESULTS/DISCUSSION

Unaveraged interface scattering strength (S_b) as a function of horizontal range (x) for the 70 kHz transducer is shown in Fig. 3a. Significant wave height is also plotted for the same time frame as the acoustic data (Fig. 3c). Weak S_b levels extending from maximum to minimum ranges in Fig. 3a are storm events.

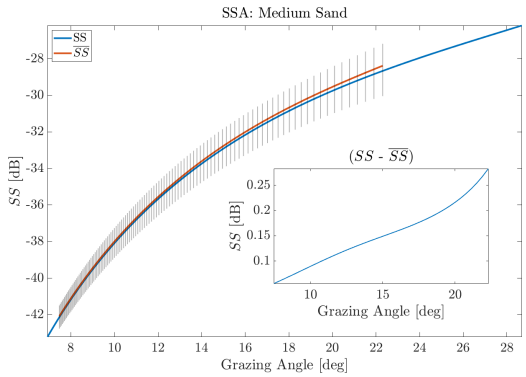

Figure 2: Bias analysis of spatial averaging technique used. The small slope approximation is represented by the blue line (SS). The orange line represents a 25 point averaging window ($\overline{SS}$). Vertical bars represent the range of SS averaged for each point. The difference between SS and $\overline{SS}$ is shown in the inset.

Large storms were frequent from January to April (Fig. 3c). Following December 25th in the S_b time series (Fig. 3a), stronger seafloor returns were observed around 6 m, 9 m, and 13 m; these were potentially bed forms that formed following large storm events (> 5 m H_s) in mid December. SS in late December and early January are about -34 dB then dropped to -37 dB in February before increasing back up to -34 dB (Fig. 3b).

Unaveraged interface scattering strength (S_b) as a function of horizontal range (x) for the 333 kHz transducer is shown in Fig. 4a. Only one mean grazing angle can be extracted from the S_b plot owing to the narrower beam width of this transducer. The time series of SS at 18° grazing angle is shown in Fig. 4b. SS seasonal trends observed at 333 kHz were mirrored by the 70 kHz data. A slow decreasing trend in SS is observed with consistent minimums around early February as seen on the fit (Fig. 4b). Following a large storm event on March 14th (Fig. 4a), S_b increased which may have been a result of biological activity roughening the surface[12]. Following lows in February SS increased and then stayed consistently around -22 dB from April onward.

SS at 70 kHz for three grazing angles ($10°, 14°, 18°$) are plotted in Fig. 5 along with significant wave height (H_s). The lowest SS values were observed in February for all frequencies and grazing angles (Fig. 5a,b,c and Fig. 4b). A study done by Pouliquen et al.[12] found that near bed hydrodynamics tends to smooth seafloor roughness at acoustically relevant scales leading to decreases in SS. Biological activity tends to roughen the seafloor at acoustically relevant scales resulting in increases of SS[12]. One possible explanation for mid-winter lows could be a higher frequency of storms during winter causing a reduction of roughness features at acoustically relevant scales[3]. Moreover, SS levels might stay low due to a seasonal dependence of the abundance of animals in this location. Comparisons of January and April SS show similar levels at all grazing angles suggesting that even though SS drops in February, it returns to pre-January levels once storm activity has reduced.

The average scattering strength during two 7-day non-stormy periods in January and April are plotted as a function of grazing angle (Fig. 6). Little difference between both periods were observed. SS values were compared to the SSA model[8] with input parameters for a medium sand[8] and $\omega_2 = 1.05e-04$. The input parameter for surface roughness (ω_2) was chosen based on best fit. The model appears to capture the angular response well with the given parameters. It is important to note that shell pieces were observed in the underwater photographs which would likely increase the SS[14]. The model does not account for scattering from shells.

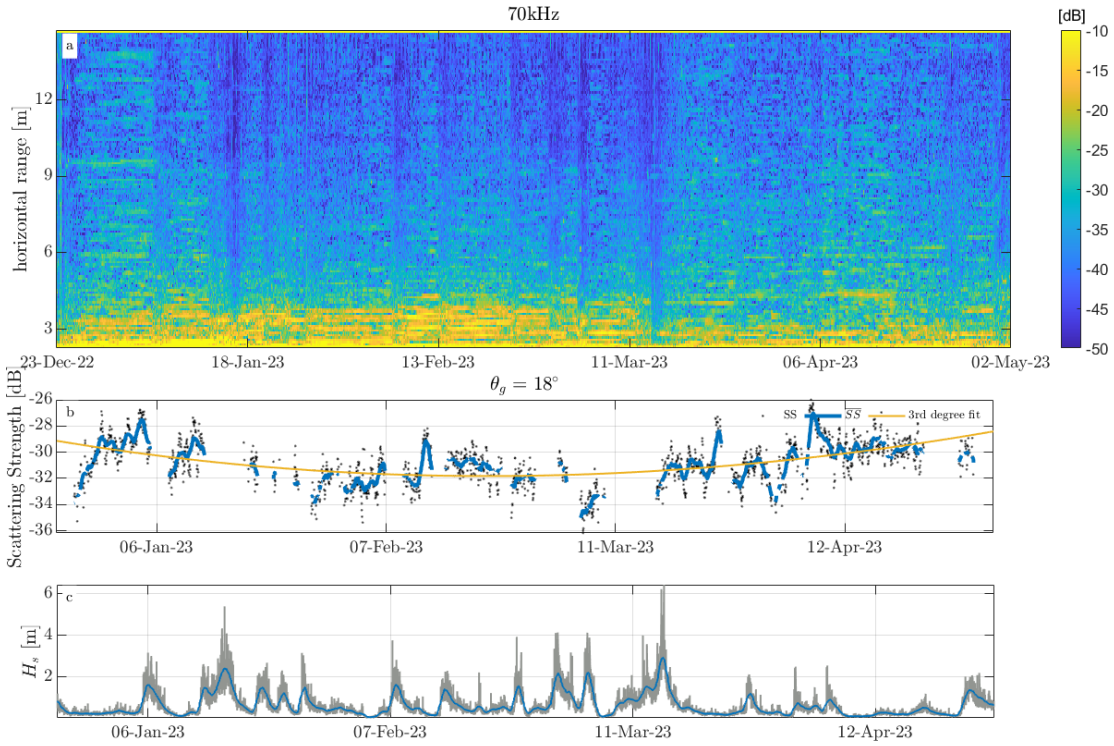

Figure 3: (a) Unaveraged interface backscattering strength, S_b, at 70 kHz as a function of horizontal distance along the seafloor x. (b) Scattering strength with dots representing hourly SS values and the blue line representing a daily moving average of SS. The yellow line is a third degree polynomial fit shown to highlight long-term fluctuations. (c) Significant wave height H_s with a daily moving average represented by the blue line.

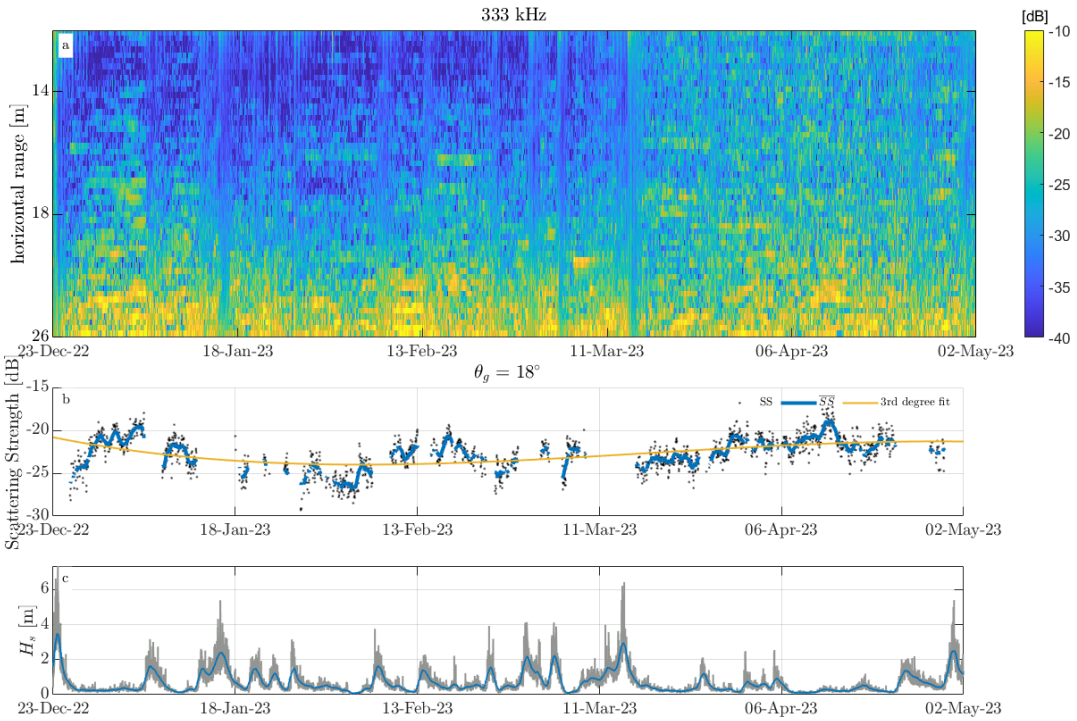

Figure 4: Same caption as Fig. 3 except for 333 kHz

4 CONCLUSION

Scattering strength (SS) was measured at two frequencies (70 kHz, 333 kHz) in a shallow water (16 m) sandy site in the Gulf of Maine for 131 consecutive days. Transducers were oriented at a nominal grazing angle of 20° and mounted approximately 2 m above the seafloor. SS values in early January were comparable to values in mid-April and onward. Mid-winter lows in SS were observed. Storm activity throughout the winter smoothing seafloor roughness elements at acoustically relevant scales is one potential explanation for mid-winter decreases in SS.

Future work will include analysis of a data set from the same location that spans September 2023 to May 2024. Monthly vessel surveys taken in the same region and using the same acoustic equipment as the tripod will also be analyzed. The vessel surveys will have results from 20°-90° grazing angle allowing for comparisons between angular response curves for the tripod and the vessel data. Comparisons between models and the data can confirm model validity, leading to an improved understanding of the temporal variability of scattering strength.

5 ACKNOWLEDGMENTS

Thank you to the Dr. Thomas Blanford, Capt. Bryan Soares and the crew of the UNH R/V Gulf Challenger for their assistance with tripod deployment and recovery.

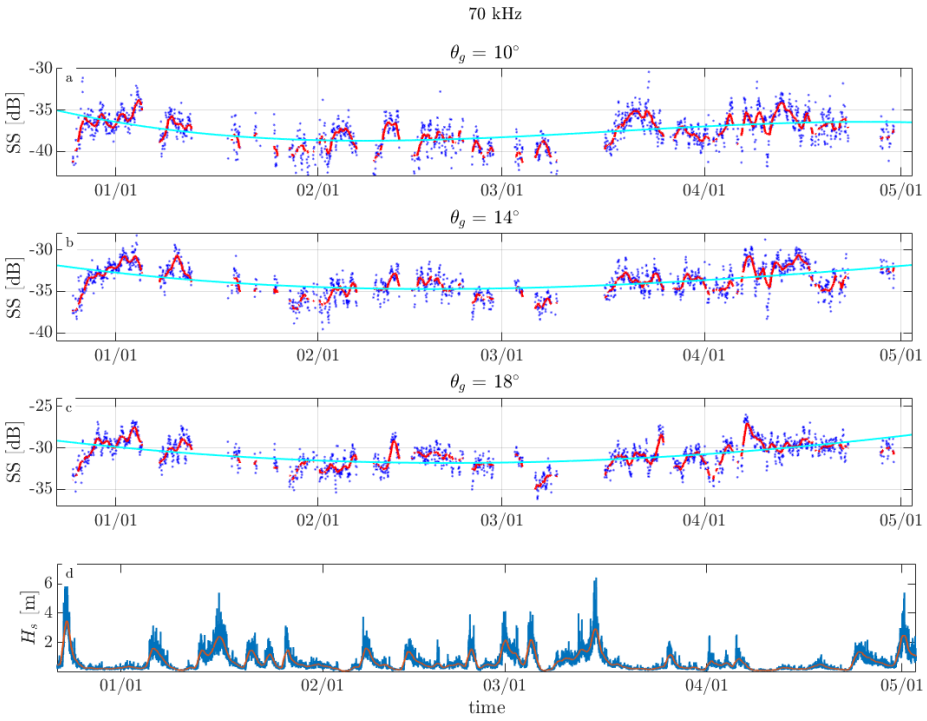

Figure 5: (a,b,c) Scattering strengths at 70 kHz for $\theta_g = 10°, 14°, 18°$. The dots represent hourly SS values and the red lines represent a daily moving average of SS. The cyan lines are third degree polynomial fits of the hourly data. (d) Significant wave height H_s with a daily moving average in red.

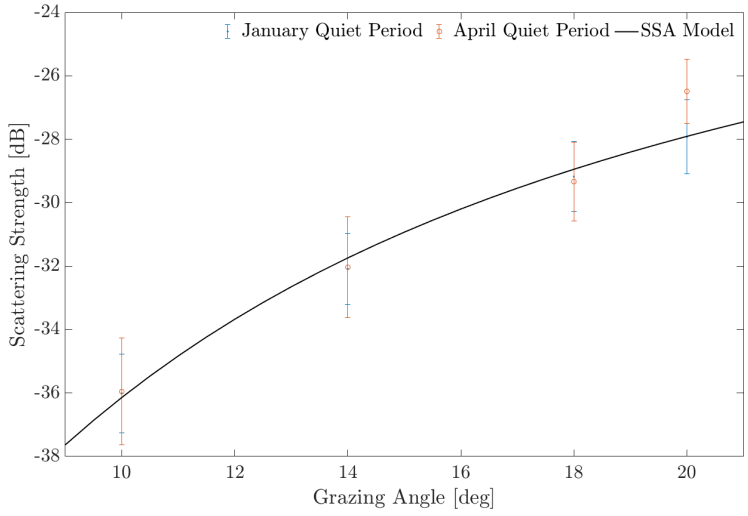

Figure 6: Angular response curve for the 70 kHz SS data for January (blue) and April (orange) quiet periods. The black line is the SSA model with parameters for a medium sand ($\omega_2 = 1.05\mathrm{e}-04$).

REFERENCES

1. D. A. Abraham. *Underwater Acoustic Signal Processing: Modeling, Detection, and Estimation*. Springer, 2019.
2. L. N. Andersen, D. Chu, N. O. Handegard, H. Heimvoll, R. Korneliussen, G. J. Macaulay, E. Ona, R. Patel, and G. Pedersen. Quantitative processing of broadband data as implemented in a scientific split-beam echosounder. *Methods Ecol. Evol.*, 15(2):317–328, 2024. doi: https://doi.org/10.1111/2041-210X.14261.
3. K. B Briggs, K. L Williams, M. D. Richardson, and D. R. Jackson. Effects of changing roughness on acoustic scattering:(1) natural changes. *Proc. Inst. Acoust.*, 23(2):375–382, 2001.
4. M. Catoire. Preliminary investigation into temporal changes in acoustic scattering from the seafloor. Master's thesis, University of New Hampshire, 2021.
5. J. G. Dworski and D. R. Jackson. Spatial and temporal variation of acoustic backscatter in the stress experiment. *Cont. Shelf Res.*, 14(10):1221–1237, 1994. ISSN 0278-4343. doi: https://doi.org/10.1016/0278-4343(94)90035-3. Sediment TRansport Events on Shelves and Slopes: STRESS.
6. J. A. Gruber and D. R. Olson. Scattering measurements of rocky seafloors using a split-beam echosounder. *JASA Express Letters*, 4(2):026001, 02 2024. ISSN 2691-1191. doi: 10.1121/10.0024755.
7. J. Hare, A. P. Lyons, and G. R. Venegas. Measurements of Temporal Change in Seafloor Scatter and its Dependence on Environmental Variability. In *Proc. 7th Underwater Acoust. Conf. & Exhibit.*, pages 121–126, 2023.
8. D. R. Jackson. High-frequency bistatic scattering model for elastic seafloors. Technical report, Washington University Seattle Applied Physics Lab, 2000.
9. D. R. Jackson and M. Richardson. *High-Frequency Seafloor Acoustics*. Springer Science & Business Media, New York, NY, 2007.
10. D. R. Jackson, K. L. Williams, and K. B. Briggs. High-frequency acoustic observations of benthic spatial and temporal variability. *Geo-Marine Letters*, 16(3):212–218, 1996. doi: https://doi.org/10.1007/BF01204511.
11. P. A. Jumars, D. R. Jackson, T. F. Gross, and C. Sherwood. Acoustic remote sensing of benthic activity: A statistical approach. *Limnol. Oceanogr.*, 41(6):1220–1241, 1996. doi: https://doi.org/10.4319/lo.1996.41.6.1220.
12. E. Pouliquen, G. Canepa, L. Pautet, and A. P. Lyons. Temporal variability of seafloor roughness and its impact on acoustic scattering. In *Proceedings of the Seventh European Conference in Underwater Acoustics ECUA2004, Delft, The Netherlands*, pages 5–8, 2004.
13. I. Schulze, M. Gogina, M. Schonke, M. L. Zettler, and P. Feldens. Seasonal change of multifrequency backscatter in three baltic sea habitats. *Frontiers in Remote Sensing*, 3, 2022. ISSN 2673-6187. doi: 10.3389/frsen.2022.956994.
14. R. F. L. Self, P. A'Hearn, P. A. Jumars, D. R. Jackson, M. D. Richardson, and K. B. Briggs. Effects of macrofauna on acoustic backscatter from the seabed: field manipulations in west sound, orcas island, washington, usa. *J. Mar. Res.*, 59(6):991–1020, 2001. doi: https://doi.org/10.1357/00222400160497742.
15. T. C. Weber and L. G. Ward. Observations of backscatter from sand and gravel seafloors between 170 and 250 kHz. *J. Acoust. Soc. Am.*, 138(4):2169–2180, 10 2015. ISSN 0001-4966. doi: 10.1121/1.4930185.